Earthquake Engineering, Tenth World Conference © 1992 Balkema, Rotterdam. ISBN 90 5410 060 5

Experimental and numerical studies on dynamic earth pressure acting on side walls of underground conduit

H.Watanabe
Saitama University, Japan
T.Suehiro
Tokyo Electric Power Co., Ltd, Japan

ABSTRACT: The ground-conduit models where model conduits of different rigidities are buried in the model ground of air dried sand compacted in a shear testing apparatus are excited with the sinusoidal motions of resonant frequencies on a shaking table. They are also simulated with FEM numerical analyses. Synthesizing both results the mechanism of development of dynamic earth pressures on the side walls of underground conduit are clarified.

1 INTRODUCTION

In the earthquake resistant design of under ground structures such as submerged tunnels, underground conduits and so on, the cross section should be examined so as to resist against earthquake load. Main part of it is horizontal earth pressure being specified to determine from Mononobe and Okabe's formulae in Japanese design standard. Above formulae were, however, originally proposed for the design of retaining wall, and are not necessarily fit to such underground structures of flexible walls as conduits. In fact, many of recent research papers point out that the horizontal earth pressures acting on underground structures relate to these displacements relative to free ground motion at each location.

The objects of this paper are to clarify the mechanism of development of horizontal earth pressures on the underground conduits and to derive a formula to predict them quantitatively through the exciting tests on ground-conduit models on a shaking table and the numerical simulations of them.

2 MODEL EXPERIMENTS AND RESULTS

One free ground model of air dried Gifu sand compacted in a shear testing apparatus and three ground-conduit composite models were excited horizontally with sinusoidal motions of resonant frequencies on a shaking table. Each composite model had 1/35 reduced scale of prototype and had been made by burying a model conduit of acrylic resin or steel plate as shown in Fig.1 in the ground model of which density ρ_G is 1.369(gr/cm^3). Accelerations at 5 points in ground and conduit as well as horizontal earth pressures at 3 points along a side wall were measured for each model. On every conduit two states were examined, one buried deeply other shallowly. Arrangement of the conduit and location of every gauge are shown in Fig.2. An example of observed response accelerations in resonance with deeply buried case and free ground is shown in Fig.3. It is seen that the response acceleration at the bottom of conduit is reduced in case 1 where the apparent shear rigidity of it is lower than the one of soil though the acceleration at ceiling of conduit is kept at the value of free ground. Besides, the response horizontal earth pressures along a side wall distribute as shown in Fig.4 at every phase of base motion in the deep case. It is seen that the dynamic earth pressure reverses in its acting direction at same phase of base motion, as shear rigidity of conduit changes from very lower (Case 1) to very higher (Case 3) than the one of surrounding soil layer, whereas such reversion does not occur in the

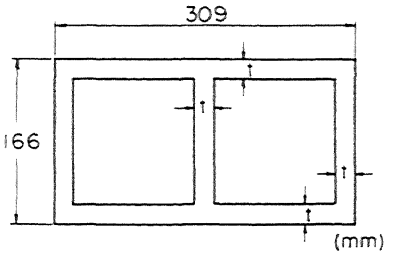

Model Case	t (mm)	Material
1	8	Acrylic Resin (A.R.)
2	20	A.R
3	16	Steel

Figure 1. Material and dimension in cross section of model conduits.

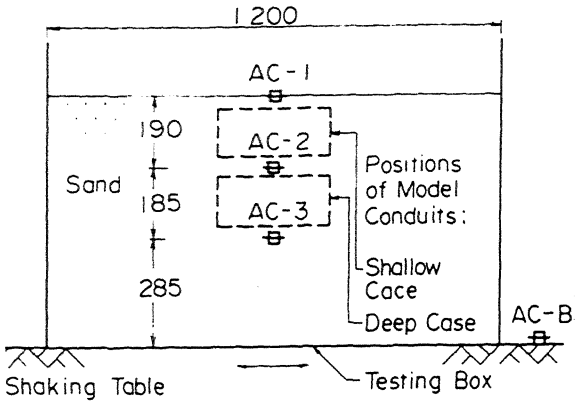

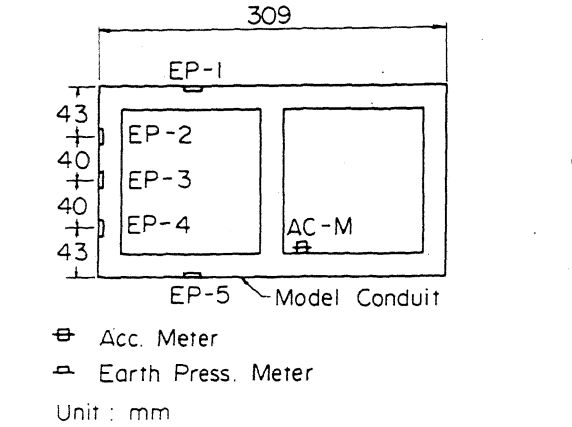

Figure 2. Arrangement of model conduits and gauges.

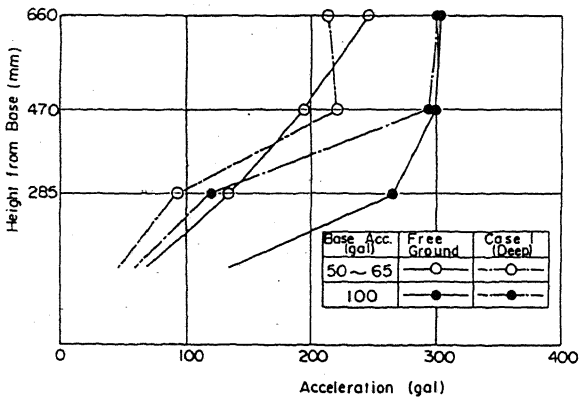

Figure 3. Distribution patterns of response accelerations in free ground and case 1.

shallowly buried case as shown in Fig. 5.

The outline of above results will be explained as follows. The shear forces transmitted from soil to the ceiling and bottom of conduit are born only partially by the conduit in the case of lower rigidity like case 1 so that the excess forces must be supported by normal stresses acting on side walls. On the contrary in the case of higher rigidity like case 3 the shear forces are insufficient to deform the conduit up to surrounding soil so that the shortage forces must be supplied by the normal stresses of inversed direction on the walls. In shallowly buried cases the shear force on the ceiling is nearly equal to zero and the deformation of conduit is caused only by the one of soil layer adjacent to side walls. The deformation of above soil depends hardly on the rigidity of conduit so that the normal stresses on side walls do not change these directions.

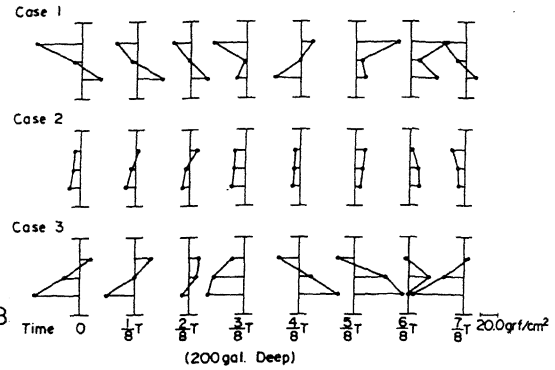

Figure 4. Time history of the distribution pattern of dynamic earth pressure (in case buried deeply and 200 gal of base motion).

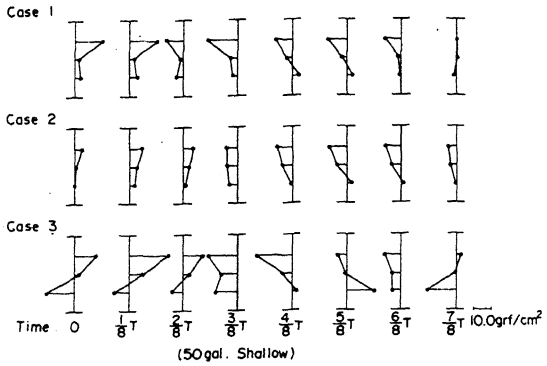

Figure 5. Time history of the distribution pattern of dynamic earth pressure (in case buried shallowly, 50 gal of base motion).

3 NUMERICAL EXPERIMENTS AND RESULTS

Above experiments were simulated with 2-D

FEM numerical models where the conduit was idealized by beam elements, ground by triangle finite elements of constant strain shape functions and joint element was inserted between each beam element and adjacent finite element as shown in Figs. 6 and 7. Dynamic constants of sand were formulated by hyperbolic model from dynamic torsion tests.

$$G/G_0=2.95\times10^{-4}/(\gamma+2.95\times10^{-4}) \quad (1)$$

$$G_0=700[(2.17-e)^2/(1+e)](\sigma_m')^{0.321} \quad (2)$$

$$h=0.337[\gamma/(\gamma+2.95\times10^{-4})] \quad (3)$$

In above model experiments, observed natural frequency of free ground was 35.9(Hz) to the intensity of 50(gal) of base motion and the simulated one with above dynamic constants was 35.6(Hz) and very close to observed one. Taking into account of lots of numerical experiments which should be carried on later, it will be convenient to proceed them with linear dynamic constants. Linear homogeneous shearing rigidity of model free ground with above natural frequency can be estimated easily and the shear strain which gives same rigidity can be obtained from Eq.(1), from which corresponding damping constant can be obtained. Thus, linear dynamic constants to the base motion of 50(gal) are defined.

$$G=123.4(\mathrm{Kgf/cm^2}),\ h=0.110 \quad (4)$$

Dynamic earth pressures were estimated as the stresses of joint elements with spring constants of 600(Kgf/cm²) for k_s and k_n.

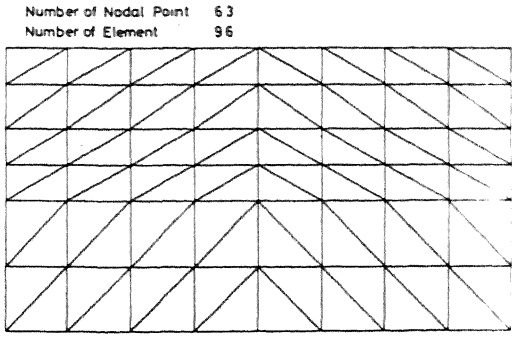

Figure 6. Finite element idealization of free ground

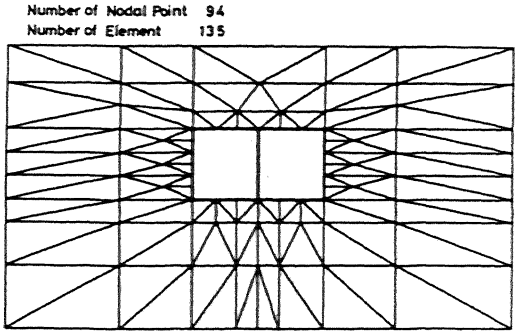

Figure 7. Finite element idealization of ground-conduit composite model

3.1 Effects of material nonlinearity of ground on dynamic earth pressures

Steady state responses by sinusoidal base motion with natural frequency in every model were obtained after the tenth period. Examples of response accelerations of free ground and case 1 along a vertical line at the time when surface acceleration becomes maximum are shown in Fig.8 for both of linear and equivalent linear cases with base motion of 50(gal) in the amplitude. It is seen that the response acceleration at bottom of conduit is reduced from the one of free ground at same point just like the exciting model tests. Because of nonhomogeneous distributions of dynamic constants the response accelerations are larger in the equivalent linear cases than in the linear ones. The response earth pressures along a side wall are, however, almost same in both cases as shown in Fig.9. With linear dynamic constants cases 1, 2 and 3 of above exciting model tests were simulated and the response earth pressures at same phases of base motion are obtained as shown in Fig.10 which shows the same result of change in the direction of earth pressure as in the tests. In order to see the effects of material nonlinearity of ground on the response earth pressures more precisely, equivalent linear

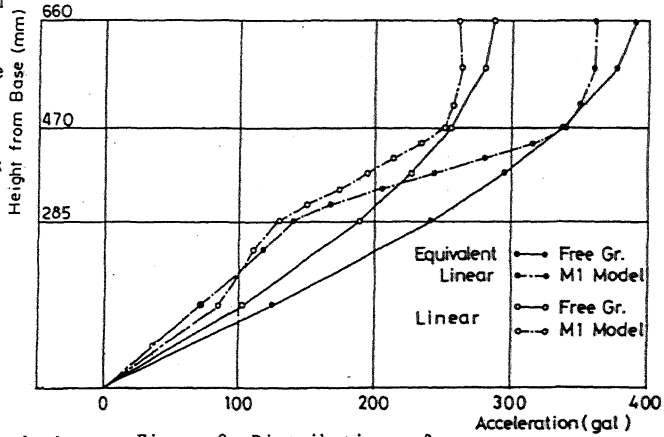

Figure 8. Distributions of response accelerations of free ground and case 1

analyses were carried on with 100, 200, 300 and 450(gal) of amplitudes of base motion and the ratio of the earth pressure obtained above to the one in linear case at each of top (S-1) and bottom (S-6) points at a side wall is plotted against the amplitude of base motion resulting in Fig.11. M-1 in Fig.

11 is the numerical model of case-1 in above model experiments and M-10 is the one of which apparent shear rigidity is 10 times as large as the one of ground. These dimensions are shown in Table 1.

As seen in Fig.11 above mentioned ratios become smaller as the intensity of base motion increases. In the case of conduit of higher rigidity the ratios are lower than unity in all range of base motion amplitude larger than 100(gal). Besides, in the range larger than 200(gal) above ratio is lower or equal to unity even in the case of conduit of lower rigidity. Thus, regarding that the intensity of base motion taken into consideration in aseismatic design of structures may be larger than 200 (gal), it may be said that the earth pressures are estimated with linear numerical analyses in safe side from view point of design.

3.2 Effects of separation and slide between conduit and soil on dynamic earth pressures

In very strong motion earthquake the discontinuity such as separation and slide between conduit and soil may occur in addition to material nonlinearity of ground mentioned above. In order to examine these effects on dynamic earth pressures, nonlinear seismic response analyses on two numerical models of M-1 and M-10 were carried on giving the constitutive relationships as shown in Fig.12 to joint elements with the sinusoidal base motion of 450(gal) in amplitude and of resonant frequencies of them and with converged dynamic constants for soil obtained from the results of the preliminary equivalent linear analyses with same base motion where joint elements with linear rigidity were allowed to neither slide nor separate. Shear strength τ_y is defined from Mohr-Coulomb criteria with following strength constants.

$c=10(gf/cm^2)$, $\phi=27.5^\circ$

Examples of calculated dynamic earth pressures being accompanied by separation are shown in Fig. 13. It may be said that separation of conduit from soil reduces the earth pressures, so that they are estimated safely with linear numerical analyses.

4 DISCUSSION ON THE MECHANISM

Let the sinusoidal base motion of a resonant frequency ω of soil layer

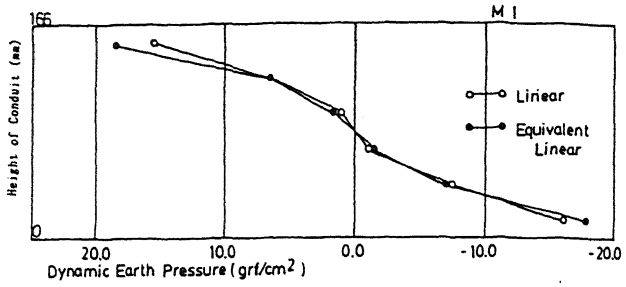

Figure 9. Dynamic earth pressures obtained from linear and equivalent linear analyses.

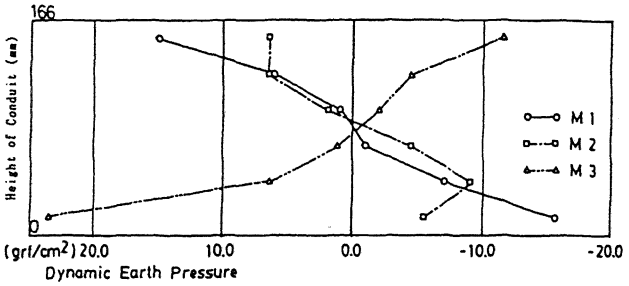

Figure 10. Change in distribution of dynamic earth pressures with rigidity of conduit.

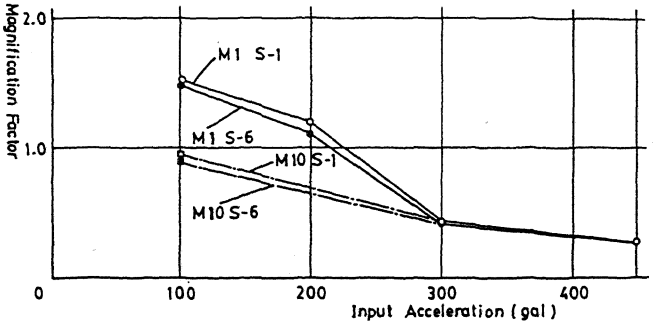

Figure 11. Ratio of earth pressure of equivalent linear case to one of linear case.

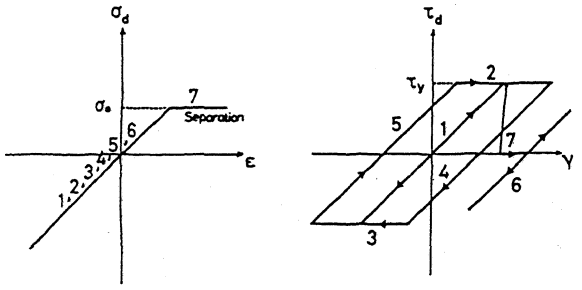

Figure 12. Constitutive relationships of joint element.

be y(t) as follows.

$$y(t)=U_0\sin\omega t \quad (5)$$

The solution of plane wave equation for the fundamental mode is given as follows.

$$u(t,z)=u_1(z)\sin(\omega t-\pi/2) \quad (6)$$

where $u_1(z)$ is given with coordinate z of which origin is set on the bottom of conduit and positive in the upper direction as follows.

$$u_1(z)=[2U_0/(\pi h)]\sin\{\pi(z+H_L)/2H\} \quad (7)$$

Here H_L is the depth of base from the bottom of conduit, H is the total depth of surface layer.

The shear stresses at positions corresponding to the ceiling and bottom are as follows.

$$\tau_U=[GU_0/(Hh)]\cdot\cos(\pi H_U/2H) \quad (8)$$

$$\tau_L=[GU_0/(Hh)]\cdot\cos(\pi H_L/2H) \quad (9)$$

where H_U is the depth of base from the ceiling of conduit. The ratio of apparent shear rigidity G^* of conduit to the one of ground is expressed as β as follows.

$$\beta=G^*/G \quad (10)$$

The displacement at the ceiling of conduit of double box frame where shearing stress τ is loaded uniformly and supported freely at the bottom is given by

$$u_2(b)=\tau ab^2(3a^2+6ab+2b^2)/[36EI(2a+b)] \quad (11)$$

2a, b and EI are the width, the height and the flexural rigidity of the framework of conduit respectively. Thus, G^* is given by

$$G^*=36EI(2a+b)/[ab(3a^2+6ab+2b^2)] \quad (12)$$

The apparent density of conduit ρ^* is given approximately as follows,

$$\rho^*=[(4a+3b)/(2ab)]\cdot\rho A \quad (13)$$

where ρ is the density of the material of conduit and 1.19(gr/cm³) in the above model conduit of acrylic resin, and A is the area of unit width times thickness of conduit.

In order to examine how the dynamic earth pressures are generated lots of numerical experiments were carried on in place of above model exciting tests. All dimensions of numerical cases are shown in Table 1. M-4 is a standard numerical model where both of apparent shearing rigidity and density are same as those of ground, that is,

$$G=G^*,\quad \rho^*=\rho_G \quad (14)$$

M-5, M-6, M-9 and M-10 are models of EI of 1/2, 2, 1/10 and 10 times as large as one of M-4 where ρA is kept constant. M-7, M-8, M-11 and M-12 are models of ρA of 1/2, 2, 1/3 and 3 times as large as one of M-4 keeping EI constant. The effect of inertial force on earth pressures is such one as shifts the average of them without the change of distribution form of them whereas the effect of β, that is, EI on them is such one as shown

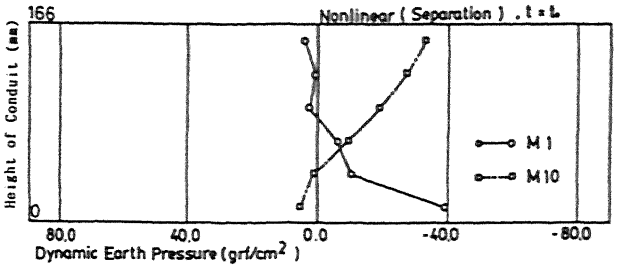

Figure 13. Dynamic earth pressures being accompanied by slide and separation.

Table 1. Numerical models and Parameters

Model No.	EI (Kgf/cm²)	ρA (gr/cm)	a (cm)	b (cm)	H (cm)	β	ρ*/ρG	Remarks
M1	1237.43	0.952	15.5	16.6	66.0	0.024	0.1511	G=123.4(Kgf/cm²)
M4	52080.0	6.3	do.	do.	do.	1.0	1.0	ρG =1.369(gr/cm³)
M5	26040.0	6.3	do.	do.	do.	0.5	1.0	β=G*/G = [36(2a+b)/ {ab(3a²+ 6ab+2b²)] · [EI/G]
M6	104160.0	6.3	do.	do.	do.	2.0	1.0	
M7	52080.0	3.15	do.	do.	do.	1.0	0.5	ρ* =(4a+3b) ρA/(2ab)
M8	52080.0	12.6	do.	do.	do.	1.0	2.0	
M9	5208.0	6.3	do.	do.	do.	0.1	1.0	
M10	520800.0	6.3	do.	do.	do.	10.0	1.0	
M11	52080.0	2.1	do.	do.	do.	1.0	0.33	
M12	52080.0	18.9	do.	do.	do.	1.0	3.0	

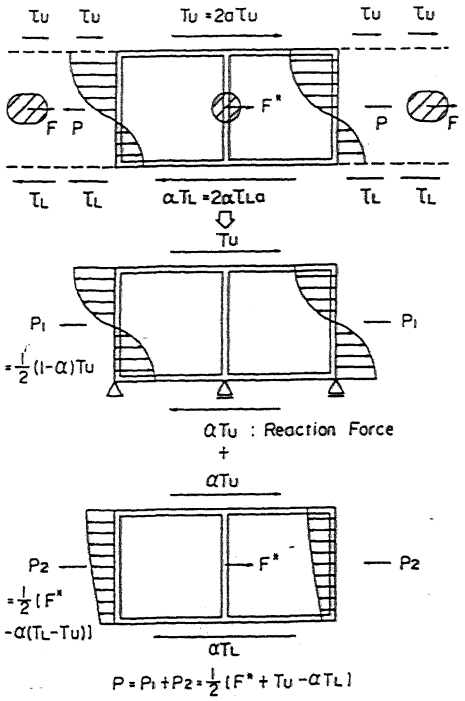

Figure 14. Concept of earth pressures bearing the share of shearing forces transmitted from the ground.

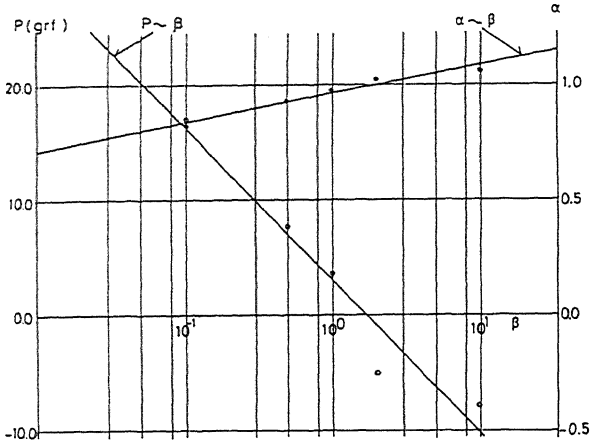

Figure 15. Relationship between P, α and β

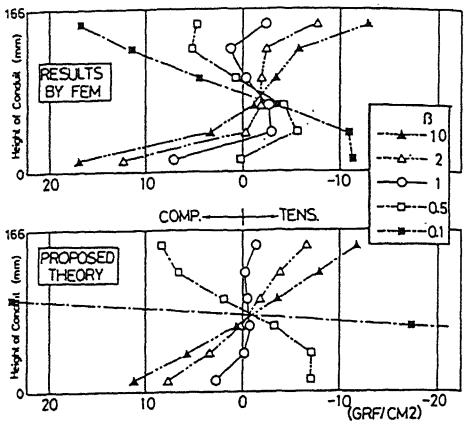

Figure 16. Predicted earth pressures and numerical ones.

in Fig. 16 just like the results obtained in the model exciting tests. Synthesizing both model exciting tests and numerical ones an idea of mechanism on generating earth pressures is obtained as shown in Fig. 14. Because of the difference in bearing ability of shear forces of conduit according to its rigidity we may regard the shear force acting on the bottom as αT_L instead of T_L and we may consider that conduit can bear only αT_U as a frame so that the residual of shear force on the ceiling, that is, $(1-\alpha)T_U$ must be born by surrounding soil as earth pressures. The total of it on a side wall is written as P_1 in Fig. 14. Remain forces are the inertial force F^* of conduit and the residual shear forces i.e. $\alpha(T_U - T_L)$ which are not necessarily in equilibrium so that we must introduce another earth pressure written as P_2 in Fig. 14. Thus total of the earth pressures is given as follows.

$$P=(1/2)[F^*+T_U-\alpha T_L] \quad (15)$$

With all forces at time when the response acceleration on ground surface becomes maximum obtained in each numerical model every term in Eq. (15) can be estimated. Plotting P and α against $\log\beta$ Fig. 15 is obtained and following relationships are derived.

$$P=A_0-B_0\log\beta,\ A_0=3.107,\ B_0=13.11 \quad (16)$$

$$\alpha=\alpha_0+\alpha_1\log\beta,\ \alpha_0=0.9637,\ \alpha_1=0.1199 \quad (17)$$

Above results sustain the validity of above mentioned idea on the mechanism generating dynamic earth pressures. The displacement $u_2^*(z)$ at any position z on a side wall due to $\alpha\tau_U$ may be given in the following equation which gives an exact one at the ceiling but has 11% error in maximum from the exact one and approximated for simplicity.

$$u_2^*(z)=[6\alpha\tau_U/(bG^*)][z^2/2-z^3/(3b)] \quad (18)$$

The earth pressure P_1 may be generated owing to the relative displacement of conduit to the one of free ground. Total earth pressure is given in Eq. (15) and the one due to relative displacement to be superposed on this may be assumed to be zero in the integration over the height of side wall. The displacement of conduit adjusted above is given by

$$u_3^*(z)=(2U_0/\pi h)[(\alpha/\beta)(\pi b/2H)\cdot\cos(\pi H/2H)\{3(z/b)^2-2(z/b)^3-1/2\}+(2H/\pi b)\{\cos(\pi H_L/2H)-\cos(\pi H_U/2H)\}] \quad (19)$$

The relative displacement is given by.

$$\Delta u(z)=u_3^*(z)-u_1(z) \quad (20)$$

All dynamic earth pressures obtained from the numerical experiments are adjusted so as to make the integration over the height be zero and expressed as σ^*. Plotting σ^* to $\Delta u(z)$ almost linear relationship is obtained except for a case of the lowest value of β. This equation is expressed as follows.

$$\sigma^*=k_z\Delta u(z),\ k_z=21450(grf/cm^2) \quad (21)$$

The total of earth pressure P is small, but its distribution is remaining unknown. Above earth pressure may depend somewhat on shear stresses in surrounding soil. So, we may assume that the earth pressure is in proportion to the rate of variation of the shear stress in free ground. Thus, we get

$$\Delta\sigma=\sigma_0\sin\pi(z+H_L)/(2H) \quad (22)$$

σ_0 is determined by the procedure that integration of $\Delta\sigma$ over the height of conduit coincides with P and is given as follows.

$$\sigma_0=P/[(2H/\pi)\{\cos(\pi H_L/2H)-\cos(\pi H_U/2H)\}] \quad (23)$$

The dynamic earth pressure at any point on a side wall is the sum of σ^* and $\Delta\sigma$, i.e.

$$\sigma=\sigma^*+\Delta\sigma \quad (24)$$

Predicted dynamic earth pressures and those obtained from FEM analyses are shown in Fig. 16. The agreement is fairly well. Generalization of the parameters k_z and α has been attained (see Watanabe 1992).

REFERENCES

Watanabe, H., 1992. A theory of dynamic earth pressures acting on underground conduit during earthquake., Proc. JSCE, No. 432/I-16, pp. 185-194.